

SHORT COMMUNICATION

 OPEN ACCESS 

## Identification of novel indole derivatives acting as inhibitors of the Keap1–Nrf2 interaction

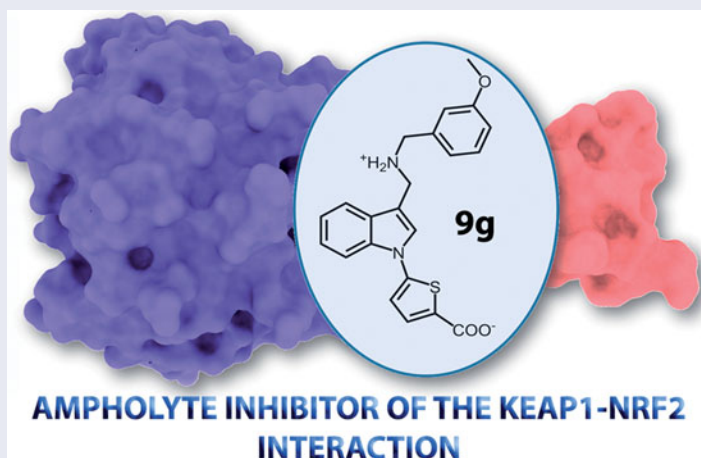
Barbara Cosimelli<sup>a</sup>, Giovanni Greco<sup>a</sup>, Sonia Laneri<sup>a</sup>, Ettore Novellino<sup>a</sup> , Antonia Sacchi<sup>a</sup>, Giorgio Amendola<sup>b</sup>, Sandro Cosconati<sup>b</sup>, Roberta Bortolozzi<sup>c</sup> and Giampietro Viola<sup>c</sup>

<sup>a</sup>Dipartimento di Farmacia, Università di Napoli “Federico II”, Naples, Italy; <sup>b</sup>Dipartimento di Scienze e Tecnologie Ambientali Biologiche e Farmaceutiche, Università degli Studi della Campania “Luigi Vanvitelli”, Caserta, Italy; <sup>c</sup>Dipartimento di Salute della Donna e del Bambino, Università di Padova, Padua, Italy

### ABSTRACT

Nine indole derivatives (**9a–i**) were tested as potential inhibitors of the Keap1–Nrf2 interaction. This class of compounds increases the intracellular levels of the transcription factor Nrf2 and the consequent expression of enzymes encoded by genes containing the antioxidant response element (ARE). In the ARE-luciferase reporter assay only **9e–g** revealed to be remarkably more active than *t*-butylhydroxyquinone (*t*-BHQ), with **9g** standing out as the best performing compound. While **9e** and **9f** are weak acids, **9g** is an ampholyte prevailing as a zwitterion in neutral aqueous solutions. The ability of **9e–g** to significantly increase levels of Nrf2, NADPH:quinone oxidoreductase 1, and transketolase (TKT) gave further support to the hypothesis that these compounds act as inhibitors of the Keap1–Nrf2 interaction. Docking simulations allowed us to elucidate the nature of the putative interactions between **9g** and Keap1.

### GRAPHICAL ABSTRACT



### ARTICLE HISTORY

Received 4 April 2019  
Revised 16 May 2019  
Accepted 20 May 2019


### KEYWORDS


Indole derivatives;  
Keap1–Nrf2 interaction;  
Keap1–Nrf2–ARE system;  
oxidative stress; antioxidant  
response element

## Introduction

The interaction between Kelch-like ECH-associated protein 1 (Keap1)<sup>1</sup> and the Nuclear Factor Erythroid 2-Related Factor 2 (Nrf2)<sup>2</sup> plays a crucial role in the homeostasis of cellular oxidative stress<sup>3</sup>. Under physiological conditions, the activity of Nrf2 as a transcription factor is negatively regulated by Keap1 through proteasomal degradation mechanisms<sup>4</sup>. An increase of the intracellular levels of reactive oxygen species (ROS) interferes with the stability of the Keap1–Nrf2 complex – situated in the cytoplasm – by oxidation of cysteine residues located in a specific domain of

Keap1. Disruption of the stability of the Keap1–Nrf2 complex triggers the release of Nrf2, allowing this protein to reach the nucleus where it behaves as a transcriptional activator of genes that contain the enhancer sequence antioxidant response element (ARE)<sup>5</sup>. As a result, several enzymes, such as NADPH:quinone oxidoreductase 1 (NQO1), heme oxygenase-1 (HO-1), glutathione S-transferase (GST), superoxide dismutase (SOD), catalase (CAT), and transketolase (TKT) are overexpressed<sup>6–8</sup>. These antioxidant enzymes reduce oxidative stress and, consequently, limit cellular damages. Thus, the Keap1–Nrf2–ARE system plays a pivotal role in

**CONTACT** Giovanni Greco  [giovanni.greco@unina.it](mailto:giovanni.greco@unina.it)  Dipartimento di Farmacia, Università di Napoli “Federico II”, Via Domenico Montesano 49, 80131, Naples, Italy

 Supplemental data for this article can be accessed at <https://doi.org/10.1080/14756366.2019.1623209>.

© 2019 The Author(s). Published by Informa UK Limited, trading as Taylor & Francis Group.

This is an Open Access article distributed under the terms of the Creative Commons Attribution License (<http://creativecommons.org/licenses/by/4.0/>), which permits unrestricted use, distribution, and reproduction in any medium, provided the original work is properly cited.

cellular metabolism and redox balance. For the above reasons, inhibitors of the Keap1–Nrf2 interaction are currently being investigated as potential drugs to treat diseases involving chronic oxidative stress, such as diabetes, cancer and neurodegenerative disorders<sup>9</sup>.

The first non-peptide small molecules disrupting the Keap1–Nrf2 interaction by binding to Keap1 with micromolar affinities were reported by Hu et al.<sup>10</sup> and Marcotte et al.<sup>11</sup> using high throughput screening methods. This latter group also solved the 3D structures of two ligand–Keap1 complexes by X-ray crystallography<sup>11</sup>. The above quoted works gave impetus to additional X-ray diffraction studies and researches aimed at identifying novel ligands of Keap1<sup>12</sup>.

According to Jiang et al.<sup>12</sup>, the Keap1 binding cavity hosting inhibitors of the Keap1–Nrf2 interaction can be divided into six subpockets (P1–P6). P1 and P2 contain protonated arginine residues (R483, R415, R380) which give rise to strong electrostatic interactions with electron-rich parts of ligands; specifically, salt bridges with carboxylate groups, H-bonds with nitro oxygens or azole nitrogens, cation– $\pi$  contacts with aromatic rings. Additional polar as well as hydrophobic interactions are established between ligands and the complementary Keap1 binding cavity. Some inhibitors of the Keap1–Nrf2 interaction, representative of the variety of a huge number of those reported in literature<sup>10–16</sup> are reported in Chart 1. They typically contain in their structures a planar or quasi-planar scaffold bearing at least one aromatic ring involved in cation– $\pi$  interactions.

Our research group has been working for several years on different series of indole derivatives each of them binding with high potency and selectivity to the benzodiazepine receptor<sup>17</sup>, the A<sub>2B</sub> adenosine receptor<sup>18</sup> and the translocator protein<sup>19</sup>. Given the commonly ascertained utility of indole as a scaffold for drug-like molecules (see compound **4** in Chart 1), we tried to identify novel indole derivatives which could act as inhibitors of the Keap1–Nrf2 interaction with the help of molecular modelling and substructure search methods. Specifically, a few indole-bearing models were superimposed on available 3D structures of inhibitors of the Keap1–Nrf2 interaction co-crystallised with Keap1. Starting from

some designed indole derivatives we identified commercially available compounds using the SciFinder<sup>20</sup> substructure search routine. Examples of the above approaches are given in the Supporting Information. The present paper describes the results of our studies.

## Results

### Chemistry

Nine indole derivatives fulfilling the pharmacophoric requirements to act as inhibitors of the Keap1–Nrf2 interaction<sup>12</sup> were selected for biological evaluation (**9a–i** reported in Chart 2). Compounds **9a–d** were synthesised (see Supporting Information), whereas **9e–i** were purchased from AKos (AKos GmbH, Steinen, Germany). Based on their acid–base properties, these compounds can be divided into three groups: (a) non-ionisable (**9a–d**); (b) acidic (**9e, f**); ampholytic (**9g–i**). We reasoned that the presence of methoxy group(s) or a methylenedioxy moiety on the benzene rings in the structures of the selected compounds might allow them to interact with Keap1 through cation– $\pi$  interactions and H-bonds. The thiophene ring featured by **9e–g** confers more conformational rigidity to the above compounds and an electron-rich ring capable to establish cation– $\pi$  interactions.

### Biology

The biology experiments are detailed in the Supporting Information. To evaluate the capability of the indole derivatives **9a–i** to inhibit the Keap1–Nrf2 interaction, we performed a cell-based luciferase reporter assay in which induction of ARE-driven luciferase activity is mediated by Nrf2. HeLa cells were transiently transfected with ARE-luciferase reporter plasmids and treated with all compounds at the concentration of 10  $\mu$ M, except for **9g** which was tested at the concentration of 5  $\mu$ M owing to its limited solubility in phosphate buffer. *t*-Butylhydroxyquinone (*t*-BHQ), one of the canonical activators of Nrf2<sup>12,21,22</sup>, was employed as a positive

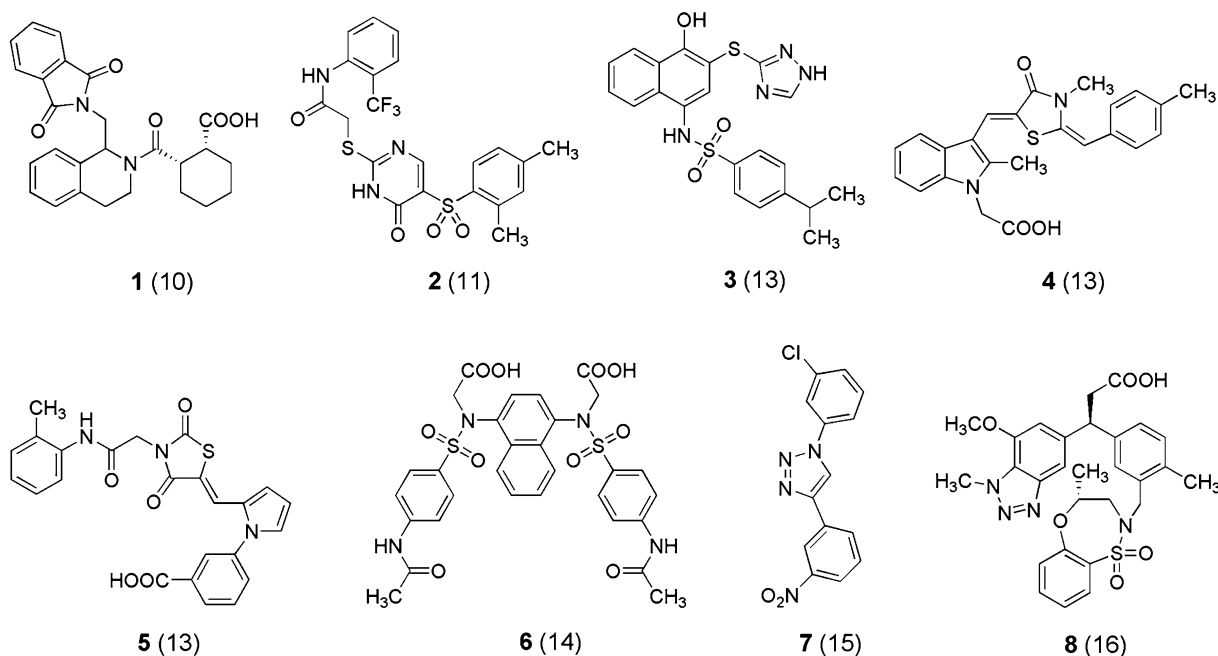


**Chart 1.** Structures of representative inhibitors of the Keap1–Nrf2 interaction. For each compound a reference is reported in parentheses. Compounds **6** and **8** exhibit nanomolar affinities for Keap1, whereas the remaining compounds bind to Keap1 with micromolar affinities.

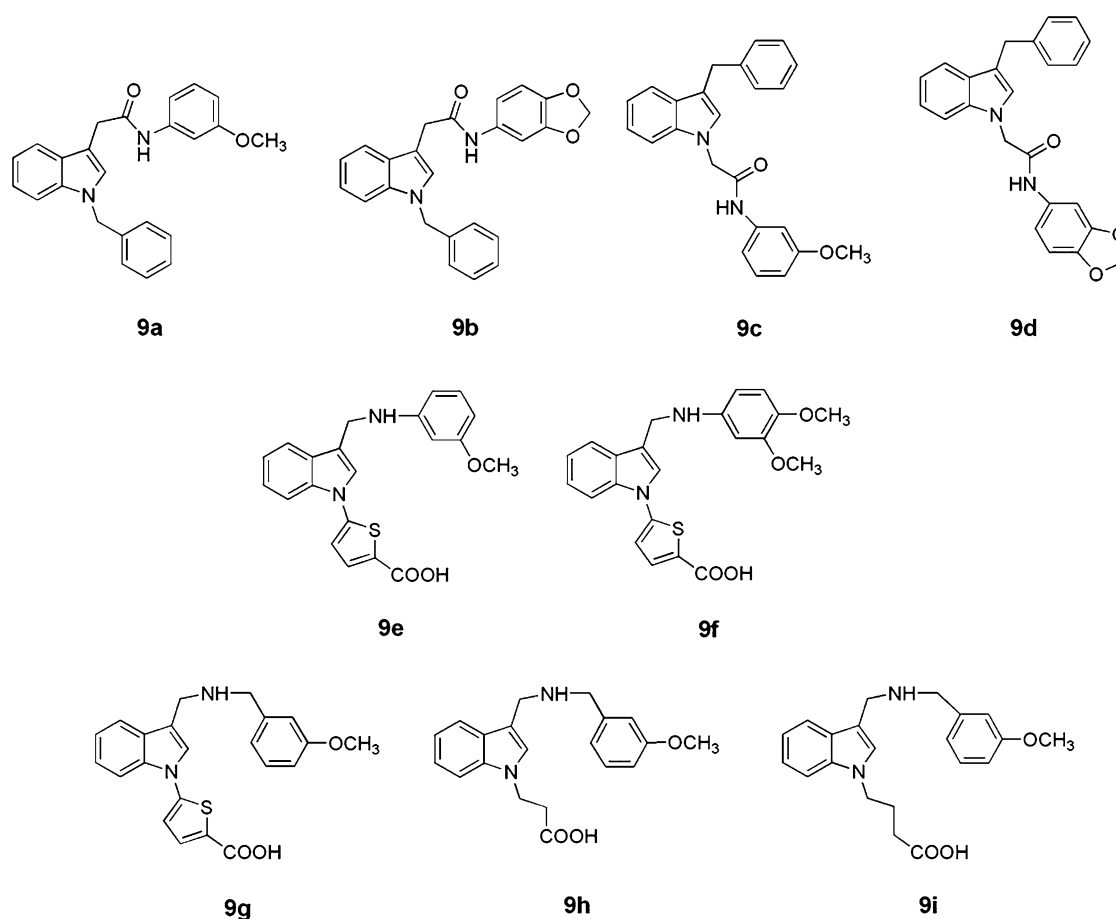


**Chart 2.** Structures of the indole derivatives selected as potential inhibitors of the Keap1–Nrf2 interaction.

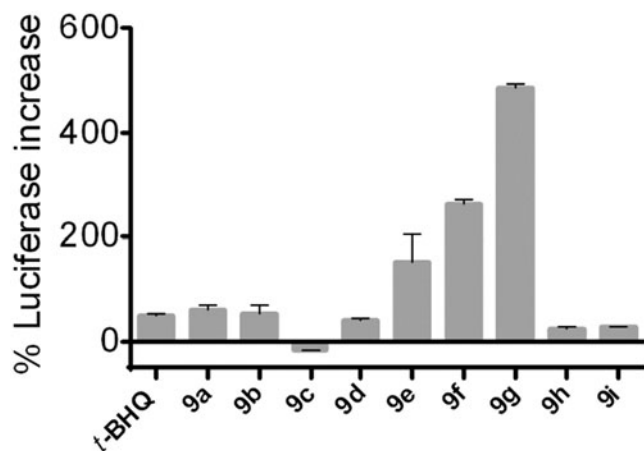


**Figure 1.** Increase of luciferase activity in HeLa cells transfected transiently with ARE-luciferase reporter plasmids after 24 h of treatment with 10  $\mu$ M of the indicated compounds, except for **9g** tested at the concentration of 5  $\mu$ M due to its limited solubility in phosphate buffer. Data are expressed as mean  $\pm$  SEM of two independent experiments performed in duplicate.

control at the concentration of 50  $\mu$ M, a value which induced in our experiments the maximum luciferase activity.

Compounds **9e**, **9f**, and **9g** increased luciferase activity by 152, 263, and 486%, respectively (Figure 1). Compared with the activity exhibited by *t*-BHQ (48% increase), the activities of **9e-g** were higher by 3.2-, 5.5-, and respectively, 10.1-folds. The remaining

compounds displayed poor activities in this assay, comparable or lower with respect to *t*-BHQ. The best performing compounds **9e-g** share a common thiophene-carboxylic moiety. Among this subset, **9e** and **9f** are acidic, whereas **9g** – by far the most active compound – is ampholytic.

To assess the inhibition of the Keap1–Nrf2 interaction exerted by **9e-g**, we evaluated the expression of Nrf2 and of two enzymes encoded by its downstream target ARE genes, namely NQO1 and TKT. HeLa cells were treated with **9e** and **9f** at the concentration of 10  $\mu$ M while **9g** was employed at the concentration of 5  $\mu$ M. We used *t*-BHQ as a reference compound at the concentration of 50  $\mu$ M. As shown in Figure 2, expression of NQO1 and of TKT remarkably increased after treatment with **9e-g**. In Figure 2, it can be appreciated a significant increase in Nrf2 levels determined by our indole derivatives, clearly much higher compared to that produced by *t*-BHQ. The original picture of the Western blot gel is reported in the Supporting Information.

Compounds **9e-g**, selected as the most active indole derivatives in the luciferase assay, were evaluated for their cytotoxicity after 72 h of incubation in human peripheral blood lymphocytes (PBLs) (Table S1). The compounds were tested either in quiescent and in proliferating PBLs (proliferation was induced by phytohematoagglutinin (PHA) as a mitogenic stimulus).

The obtained data indicate that the above compounds can be considered safe for human cells. In the absence of PHA, **9e, f** exhibited  $GI_{50}$  values greater than 100  $\mu$ M, while **9g** showed  $GI_{50}$  values greater than 5  $\mu$ M (higher concentrations of this compound could not be used due to its limited solubility in phosphate

buffer). Compounds **9e**, **f** slightly increased their cytotoxicity in proliferating PBLs showing  $GI_{50}$  values of  $61.0\ \mu\text{M}$  and, respectively,  $84.9\ \mu\text{M}$ . Compound **9g** killed 6 and 10% of quiescent and, respectively, proliferating PBLs.

### Molecular modelling

The potential interactions of **9g** with Keap1 were modelled *in silico* by docking simulations. Details of these calculations are available in the Supporting Information. Compound **9g** was treated as a zwitterion, as this species prevails to a significant extent either in neutral aqueous solutions or in the essentially polar environment of the Keap1 binding cavity. As represented in Figures 3 and 4, in our docking model the ligand occupies the central cavity of Keap1 with the carboxylate group pointing outwards and the

rest of the molecule extending into the central channel of the protein. Based on the partition of the Keap1 binding cavity proposed by Jiang et al.<sup>12</sup> into subpockets P1–P6, **9g** seemingly occupies mainly P1 and part of P2 and P3, taking into account that arginine 415 is located at the border of P1 and P2.

Several strong electrostatic ligand–protein interactions take place: the carboxylate of **9g** forms a salt bridge with the arginine 483 side chain and a charge-reinforced H-bond with the P1 serine 508 side chain; the thiophene ring of the ligand establishes a cation– $\pi$  interaction with the arginine 415 side chain (subpockets P1 and P2). Weaker hydrophobic interactions contribute to the ligand–protein affinity through favorable contacts between the indole nucleus of the ligand with the P3 alanine 556 methyl group and the arginine 415 dimethylene fragment.

The (*m*-methoxy)benzylaminomethyl substituent, in its protonated state, points deep down into the central Keap1 channel where it establishes hydrophobic interactions with valine 512 and leucine 472 side chains and a H-bond between the *m*-methoxy oxygen and the leucine 472 backbone NH.

The results of our theoretical calculations suggest that the thiophene ring featured by **9e–g**, engaged in a strong cation– $\pi$  interaction, is responsible for their considerable activities as inducers of antioxidant enzymes. This hypothesis is consistent with the much lower activities exhibited by **9h** and **9i** in which a dimethylene and, respectively, a trimethylene chain – in place of the thiophene moiety – bear a carboxyl group. However, the entropic advantage offered by the thiophene ring in reducing the conformational freedom of **9e–g** with respect to **9h**, **i** cannot be ruled out.

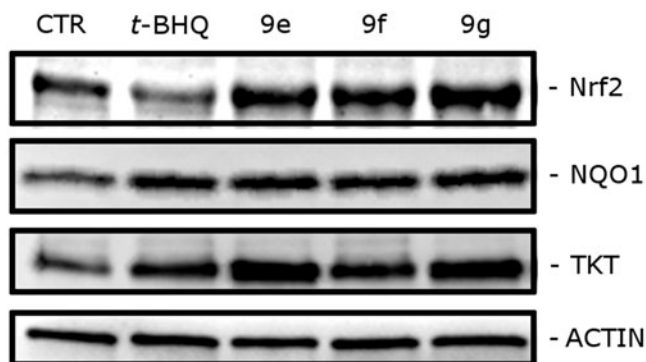


**Figure 2.** Western blot analysis of Nrf2, NQO1 and TKT after 24 h of treatment of HeLa cells with the indicated compounds. Compounds **9e** and **9f** were used at the concentration of  $10\ \mu\text{M}$ , whereas **9g** was used at the concentration of  $5\ \mu\text{M}$  due to its limited solubility in phosphate buffer. *t*-BHQ was used at the concentration of  $50\ \mu\text{M}$  as a positive control. To confirm equal protein loading, each membrane was stripped and reprobed with anti- $\beta$ -actin antibody.

### Discussion

The results of the biological experiments and the consistency of our model of the **9g**-Keap1 complex with SARs suggest that **9e–g** act as inhibitors of the Keap1–Nrf2 interaction. These three

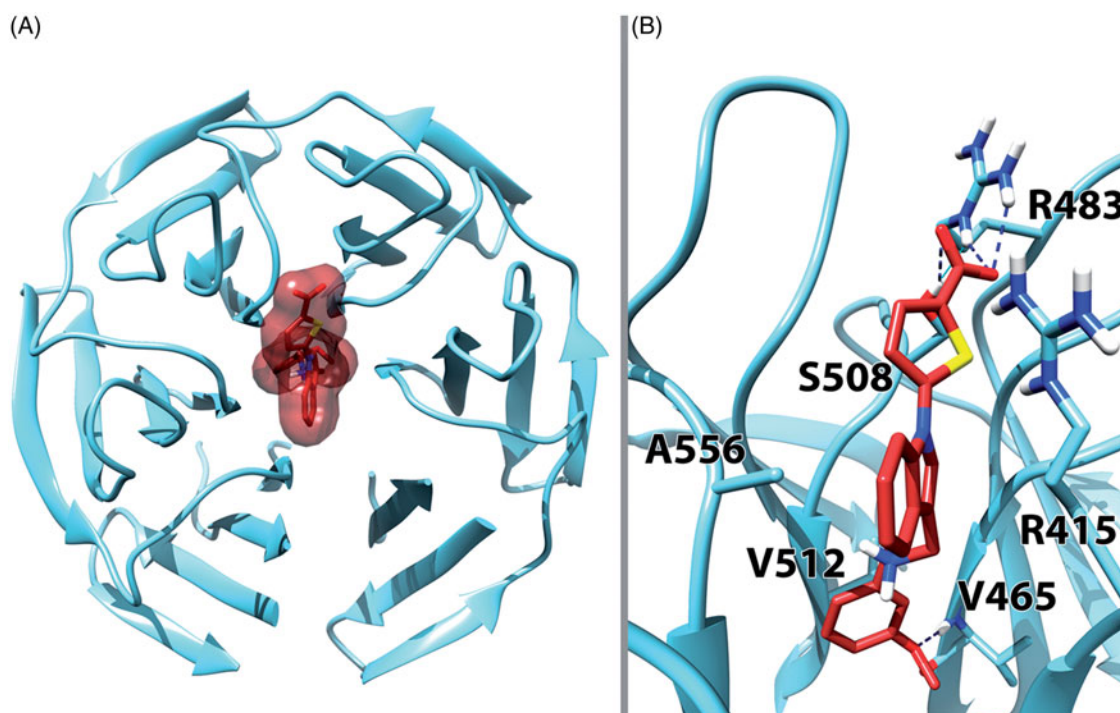


**Figure 3.** Top (A) and front view (B) of the predicted binding conformation of **9g** in complex with Keap1 extracted from the X-ray structure having PDB code 4L7B<sup>20</sup>. In panel A, the protein is represented as cyan ribbons while the ligand as brown sticks and transparent surface. In panel B, the protein is represented as cyan sticks and ribbons while the ligand as red sticks. H-bond interactions are evidenced with dashed blue lines.



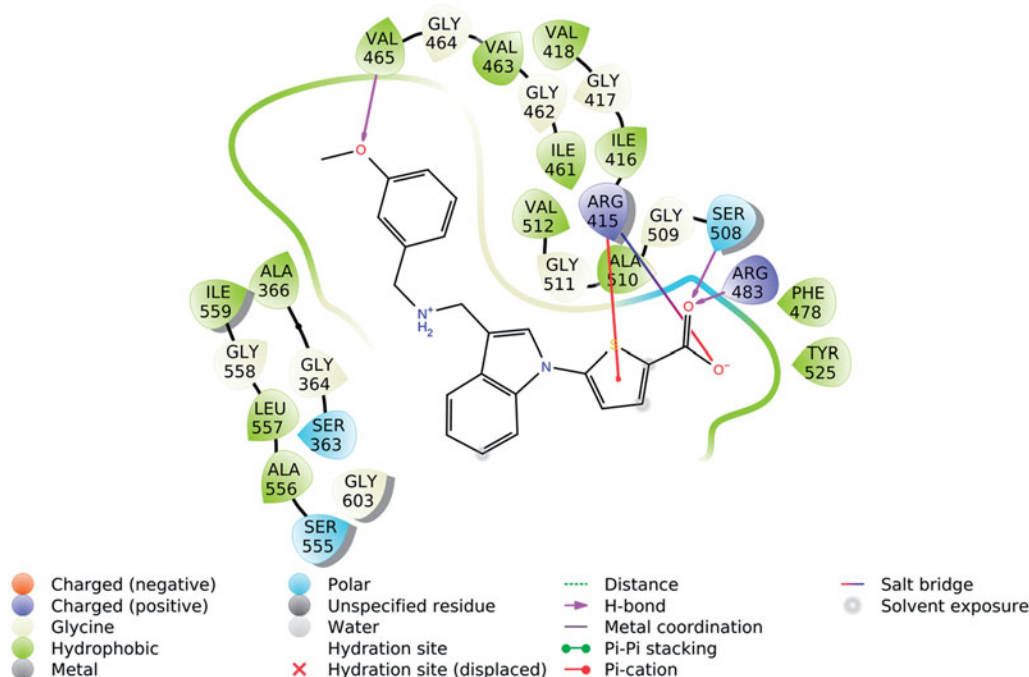


**Figure 4.** 2D scheme of interaction between **9g** docked pose and Keap1 corresponding to the docking model depicted in Figure 3.

compounds share a thiophene-carboxylate moiety which gives rise to putative strong electrostatic interactions with arginine 483 and serine 508 of Keap1 and, additionally, limits conformational freedom.

Acidic inhibitors of the Keap1–Nrf2 interaction bearing carboxylic groups exist in aqueous neutral solution mainly as anionic species. This has been considered an obstacle to translocation into cells<sup>15,23</sup>. To circumvent such a problem, bioisosteric replacements of a carboxylic group with a tetrazole ring<sup>24</sup> or a nitro group<sup>16</sup> have been attempted, yielding compounds which retained high affinity for Keap1 and exhibited improved activity in cell-based experiments. Compound **9g** stands out as the most active indole derivatives among those investigated. To our knowledge, **9g** represents the first inhibitor of the Keap1–Nrf2 interaction with ampholytic properties.

Several physicochemical and pharmacokinetic properties of **9a-i** were calculated using the Maestro QikProp tool<sup>25</sup> (Table S1). The drug-likeness of the compounds is indeed confirmed by these data that show a negligible number of Lipinski Rule of 5 and Jorgensen Rule of 3 violations, good oral absorption and a prevalently lipophilic profile for each of them.

The data reported in the present paper, together with the docking model of **9g**–Keap1 complex, will be exploited for continuing the design and the synthesis of novel indole derivatives as inhibitors of the Keap1–Nrf2 interaction.

## Acknowledgements

The authors thank Professor Roland Wolf (University of Dundee) for the generous gift of ARE-luciferase reporter plasmids.

## Disclosure statement

No potential conflict of interest was reported by the authors.

## ORCID

Ettore Novellino <http://orcid.org/0000-0002-2181-2142>

## References

- Itoh K, Wakabayashi N, Katoh Y, et al. Keap1 represses nuclear activation of antioxidant responsive elements by Nrf2 through binding to the amino-terminal Neh2 domain. *Genes Dev* 1999;13:76–86.
- Moi P, Chan K, Asunis I, et al. Isolation of NF-E2-related factor 2 (Nrf2), a NF-E2-like basic leucine zipper transcriptional activator that binds to the tandem NF-E2/AP1 repeat of the beta-globin locus control region. *Proc Natl Acad Sci USA* 1994;91:9926–30.
- Nguyen T, Sherratt PJ, Pickett CB. Regulatory mechanisms controlling gene expression mediated by the antioxidant response element. *Annu Rev Pharmacol Toxicol* 2003;43: 233–60.
- Kobayashi A, Kang MI, Watai Y, et al. Oxidative and electrophilic stresses activate Nrf2 through inhibition of ubiquitination activity of Keap1. *Mol Cell Biol* 2006;26:221–9.
- Rushmore TH, Morton MR, Pickett CB. The antioxidant responsive element. Activation by oxidative stress and identification of the DNA consensus sequence required for functional activity. *J Biol Chem* 1991;266:11632–9.
- Dinkova-Kostova AT, Talalay P. Direct and indirect antioxidant properties of inducers of cytoprotective proteins. *Mol Nutr Food Res* 2008;52:S128–S138.
- Zhu H, Itoh K, Yamamoto M, et al. Role of Nrf2 signaling in regulation of antioxidants and phase 2 enzymes in cardiac fibroblasts: protection against reactive oxygen and nitrogen species-induced cell injury. *FEBS Lett* 2005;579:3029–36.
- Xu I-J, Lai R-H, Lin S-H, et al. Transketolase counteracts oxidative stress to drive cancer development. *Proc Natl Acad Sci USA* 2016;113:E725–E734.

9. Magesh S, Chen Y, Hu L. Small molecule modulators of Keap1 – Nrf2 – ARE pathway as potential preventive and therapeutic agents. *Med Res Rev* 2012;32:687–726.
10. Hu L, Magesh S, Chen L, et al. Discovery of a small-molecule inhibitor and cellular probe of Keap1-Nrf2 protein-protein interaction. *Bioorg Med Chem Lett* 2013;23:3039–43.
11. Marcotte D, Zeng W, Hus JC, et al. Small molecules inhibit the interaction of Nrf2 and the Keap1 Kelch domain through a non-covalent mechanism. *Bioorg Med Chem* 2013;21:4011–9.
12. Jiang Z-Y, Lu M-C, You Q-D. Discovery and development of Kelch-like ECH-associated protein 1. Nuclear factor erythroid 2-related factor 2 (Keap1:Nrf2) protein – protein interaction inhibitors: achievements, challenges, and future directions. *J Med Chem* 2016;59:10837–58.
13. Zhuang C, Narayanapillai S, Zhang W, et al. Rapid identification of Keap1 – Nrf2 small-molecule inhibitors through structure-based virtual screening and hit-based substructure search. *J Med Chem* 2014;57:1121–6.
14. Jiang ZY, Xu LL, Lu MC, et al. Structure-activity and structure-property relationship and exploratory in vivo evaluation of the nanomolar Keap1 – Nrf2 protein-protein interaction inhibitor. *J Med Chem* 2015;58:6410–21.
15. Bertrand HC, Schaap M, Baird L, et al. Design, synthesis, and evaluation of triazole derivatives that induce Nrf2 dependent gene products and inhibit the Keap1 – Nrf2 protein-protein interaction. *J Med Chem* 2015;58:7186–94.
16. Davies TG, Wixted WE, Coyle JE, et al. Monoacidic inhibitors of the Kelch-like ECH-associated protein 1: nuclear factor erythroid 2-related factor 2 (Keap1:Nrf2) protein – protein interaction with high cell potency identified by fragment-based discovery. *J Med Chem* 2016;59:3991–4006.
17. Cosimelli B, Cosconati S, Marinelli L, et al. From the pharmacophore to the homology model of the benzodiazepine receptor: the indolyglyoxylamides affair. *Curr Top Med Chem* 2012;12:321–32.
18. Trincavelli ML, Giacomelli C, Daniele S, et al. Allosteric modulators of human A<sub>2B</sub> adenosine receptor. *Biochim Biophys Acta* 2014;1840:1194–203.
19. Barresi E, Agostino B, Taliani S, et al. Deepening the topology of the translocator protein binding site by novel N,N-dialkyl-2-arylindol-3-ylglyoxylamides. *J Med Chem* 2015;58:6081–92.
20. Gabrielson SW. SciFinder. *J Med Libr Assoc* 2018;106:588–90.
21. Smirnova NA, Haskew-Layton RE, Basso M, et al. Development of Neh2-luciferase reporter and its application for high throughput screening and real-time monitoring of Nrf2 activators. *Chem Biol* 2011; 18:752–65.
22. Wu KC, McDonald PR, Liu J, et al. Screening of natural compounds as activators of the Keap1-Nrf2 pathway. *Planta Med* 2014;80:97–104.
23. Jnoff E, Albrecht C, Barker JJ, et al. Binding mode and structure-activity relationships around direct inhibitors of the Nrf2-Keap1 complex. *ChemMedComm* 2014;9:699–705.
24. Lu MC, Tan S-J, Ji J-A, et al. Polar recognition group study of Keap1 – Nrf2 protein – protein interaction inhibitors. *ACS Med Chem Lett* 2016;7:835–40.
25. Schrödinger Release 2018-3: Maestro. New York, NY: Schrödinger, LLC; 2018.